Published in final edited form as:
*Sci Transl Med*. 2013 November 27; 5(213): 213ra164. doi:10.1126/scitranslmed.3007148.

# HIV-1 Vpr Induces Adipose Dysfunction in Vivo Through Reciprocal Effects on PPAR/GR Co-Regulation

**Neeti Agarwal**[1,*], **Dinakar Iyer**[1,*], **Sanjeet G. Patel**[1,†], **Rajagopal V. Sekhar**[1,2], **Terry M. Phillips**[3], **Ulrich Schubert**[4], **Toni Oplt**[1], **Eric D. Buras**[1,‡], **Susan L. Samson**[1,2], **Jacob Couturier**[5], **Dorothy E. Lewis**[5], **Maria C. Rodriguez-Barradas**[6], **Farook Jahoor**[7], **Tomoshige Kino**[3], **Jeffrey B. Kopp**[8], and **Ashok Balasubramanyam**[1,2,§]

[1]Translational Metabolism Unit, Diabetes Research Center, Division of Diabetes, Endocrinology and Metabolism, Baylor College of Medicine, Houston, TX 77030, USA.

[2]Endocrine Service, Ben Taub General Hospital, Houston, TX 77030, USA.

[3]National Institutes of Health, Bethesda, MD 20892, USA.

[4]University of Erlangen, Erlangen 91052, Germany.

[5]Division of Infectious Diseases, Department of Medicine, University of Texas Health Science Center, Houston, TX 77030, USA.

[6]Section of Infectious Diseases, Veteran's Affairs Medical Center, Baylor College of Medicine, Houston, TX 77030, USA.



[§]Corresponding author. ashokb@bcm.edu.
[*]These authors contributed equally to this work.
[†]Present address: Department of Surgery, UCLA Medical Center, Los Angeles, CA 90095, USA.
[‡]Present address: Department of Medicine, University of Michigan, Ann Arbor, MI 48109, USA.

**SUPPLEMENTARY MATERIALS**

www.sciencetranslationalmedicine.org/cgi/content/full/5/213/213ra164/DC1

Fig. S1. Plasma Vpr levels in mice injected with sVpr.
Fig. S2. Expression of adiponectin and aP2 in PGF and IF of Vpr-Tg.
Fig. S3. Gating strategy for flow cytometry.
Fig. S4. Vpr does not block differentiation genes in 3T3-L1 72 hours after differentiation induction.
Fig. S5. Hyperglycemia and hypertriglyceridemia in Vpr-Tg.
Fig. S6. Paracrine effect of Vpr.
Table S1. Vpr in human liver and adipose tissue.
Table S2. Palmitate flux in a second line of Vpr-Tg..
Table S3. Twenty-four–hour calorimetry.
Table S4. Mouse weight and food intake in Vpr-Tg and sVpr-treated mice.
Table S5. Primer sequences for ChIP qPCR.
Reference (*49*)

**Author contributions:** N.A. and D.I. performed all mouse tissue and cell experiments with assistance from T.O.; S.G.P. designed critical experiments and provided technical guidance; R.V.S. designed, optimized, and performed mouse infusion studies, plasma derivatization, MS, and calorimetry; T.M.P. performed Vpr measurements by ICE; U.S. provided mouse mAbs for Vpr detection, synthesized and conducted quality assessment of sVpr, and provided wild-type and Vpr-deficient HIV NL4.3; E.D.B. performed immunohistochemistry; S.L.S. performed glucose tolerance tests and optimized qPCR; J.C. and D.E.L. performed flow cytometry; M.C.R.-B. obtained serum samples and clinical data from untreated/NRTI-treated HIV patients; F.J. performed MS; T.K. constructed wild-type and mutant Vpr plasmids and provided advice on GR-related methods; J.B.K. engineered Vpr-Tg and provided advice on PPAR$\gamma$ -related methods; A.B. conceived the project, obtained funding, designed and supervised the experiments, and drafted the manuscript. All authors were involved in data interpretation and manuscript revision.

**Competing interests:** J.B.K. is author on a patent on the use of the mAb to Vpr. (US patent application number 11/630,880; "Monoclonal antibodies to HIV-1 andmethods of using same".) The other authors declare that they have no competing interests.

[7]Children's Nutrition Research Center, Department of Pediatrics, Baylor College of Medicine, Houston, TX 77030, USA.

[8]Kidney Disease Section, National Institute of Diabetes and Digestive and Kidney Diseases, National Institutes of Health, Bethesda, MD 20892, USA.

## Abstract

Viral infections, such as HIV, have been linked to obesity, but mechanistic evidence that they cause adipose dysfunction in vivo is lacking. We investigated a pathogenic role for the HIV-1 accessory protein viral protein R (Vpr), which can coactivate the glucocorticoid receptor (GR) and co-repress peroxisome proliferator–activated receptor γ (PPARγ) in vitro, in HIV-associated adipose dysfunction. Vpr circulated in the blood of most HIV-infected patients tested, including those on antiretroviral therapy (ART) with undetectable viral load. Vpr-mediated mechanisms were dissected in vivo using mouse models expressing the Vpr transgene in adipose tissues and liver (Vpr-Tg) or infused with synthetic Vpr. Both models demonstrated accelerated whole-body lipolysis, hyperglycemia and hypertriglyceridemia, and tissue-specific findings. Fat depots in these mice had diminished mass, macrophage infiltration, and blunted PPARγ target gene expression but increased GR target gene expression. In liver, we observed blunted PPARα target gene expression, steatosis with decreased adenosine monophosphate– activated protein kinase activity, and insulin resistance. Similar to human HIV-infected patients, Vpr circulated in the serum of Vpr-Tg mice. Vpr blocked differentiation in preadipocytes through cell cycle arrest, whereas in mature adipocytes, it increased lipolysis with reciprocally altered association of PPARγ and GR with their target promoters. These results delineate a distinct pathogenic sequence: Vpr, released from HIV-1 in tissue reservoirs after ART, can disrupt PPAR/GR co-regulation and cell cycle control to produce adipose dysfunction and hepatosteatosis. Confirmation of these mechanisms in HIV patients could lead to targeted treatment of the metabolic complications with Vpr inhibitors, GR antagonists, or PPARγ/PPARα agonists.

## INTRODUCTION

Viral infections are linked to obesity (1) and fatty liver (2), but evidence that they cause adipose dysfunction is correlative (3). In vivo mechanisms whereby viruses induce adipocyte defects in human adipose disorders have not been reported. HIV patients manifest adipose dysfunction characterized by accelerated lipolysis, lipoatrophy in some depots and lipohypertrophy in others, hepatosteatosis, dyslipidemia, insulin resistance, and hyperglycemia. Antiretroviral therapy (ART) drugs have been implicated in some abnormalities (4). However, adverse effects of ART cannot explain key aspects of the phenotype (5); for example, hypertriglyceridemia was noted before the ART era (6), and decreased body fat (7), altered fat distribution (8), and abnormal adipose gene expression (9, 10) occur in untreated patients. Thus, HIV-1 per se could cause adipose dysfunction and associated metabolic defects. In vivo demonstration of these defects and their mechanisms would provide critical proof of a viral etiology for lipodystrophy or obesity.

Viral protein R (Vpr), an HIV-1 accessory protein, functions in virion assembly, preintegration complex translocation, nucleocytoplasmic shuttling, and transcriptional

regulation of the HIV-1 long terminal repeat and host genes (11). Three effects, demonstrated in vitro, could be relevant to adipose metabolism: Vpr (i) potentiates glucocorticoid receptor (GR)–mediated transcription via an LQQLL nuclear receptor co-regulator motif (12, 13); (ii) co-represses peroxisome proliferator– activated receptor γ (PPARγ)–mediated transcription (14); and (iii) induces $G_2$-M cell cycle arrest and apoptosis in infected T cells (15). GR coactivation and PPARγ co-repression in adipocytes and hepatocytes could cause hyperlipolysis and insulin resistance, whereas $G_2$-M arrest in preadipocytes could block differentiation, leading to lipoatrophy.

Two challenges to a plausible role for Vpr in adipose and hepatic dysfunction in HIV patients are as follows: (i) HIV-1 does not infect adipocytes or hepatocytes, so how could Vpr enter these cells? (ii) Lipoatrophy, dyslipidemia, and insulin resistance occur in patients receiving ART with undetectable viral load (VL), so what could be the source of Vpr in these patients? Several characteristics of Vpr could overcome these difficulties. Vpr can be released from HIV-infected cells and circulate independently (16). Moreover, Vpr is produced by replication-deficient HIV-1 and even during inhibition of viral replication by protease inhibitors (15), so it could be released from HIV-1 sequestered in tissue reservoirs in ART-treated patients. Finally, Vpr can transduce cells in a receptor- and energy-independent manner and localize in the cytosol, nucleus, and mitochondria (14, 16).

We hypothesized that virion-free Vpr, with the ability to transduce adipose and hepatic cells, persists in the circulation of HIV patients after treatment with “viral-suppressive” ART and is sufficient to produce the HIV-associated metabolic phenotype through PPARγ co-repression, GR coactivation, and cell cycle arrest in adipose and hepatic tissues. We tested these hypotheses by measuring Vpr in the circulation of HIV-infected patients on ART and specifying Vpr-mediated pathogenic mechanisms in two mouse models: transgenic (expressing Vpr in adipose tissues and liver) and pharmacologic (designed to measure the effects of circulating Vpr).

## RESULTS

### Vpr circulates in the blood of ART-treated HIV patients with undetectable VL

We measured Vpr by immunoaffinity capillary electrophoresis (ICE) in masked serum samples from HIV-negative persons ($n = 20$) and three HIV-infected groups: (i) ART-naïve ($n = 25$), (ii) on nucleoside reverse transcriptase inhibitors (NRTIs) only ($n = 61$), and (iii) on combination ART (cART, $n = 70$), of whom 25 had undetectable VL. Ninety-six percent of the HIV patients (88% on ART with undetectable VL) had detectable (true-positive) serum Vpr (Fig. 1A). These data indicate that Vpr produced by HIV-1 persisting in reservoirs can be released into the circulation. Serum Vpr ranges overlapped in the HIV-positive groups; the median value was lower in the cART group than in the treatment-naïve group. There was no correlation between Vpr level and VL among untreated or NRTI-only patients. Vpr was identified in adipose tissues and liver obtained at autopsy of two HIV-infected, but not of three HIV-uninfected, persons (table S1).

### Vpr expressed in adipose tissues and liver circulates in the blood of transgenic mice (Vpr-Tg)

Vpr mRNA was detected in adipose tissue and liver of Vpr-Tgmice, which express Vpr under the control of the phosphoenolpyruvate carboxykinase (PEPCK) promoter (Fig. 1B). Expression of Vpr was weaker in liver than in adipose tissue, likely because of Vpr's ability to blunt the expression of PEPCK (see below). ICE demonstrated Vpr in the sera of Vpr-Tg mice [194 ± 7 pg/ml (mean ± SE)], showing that Vpr produced in tissues is released into the bloodstream (Fig. 1C). To generate the pharmacologic model, we defined the pharmacokinetics of synthetic Vpr (sVpr) in wild-type mice using intraperitoneal injections. The serum half-life of sVpr was short (6 to 12 hours, fig. S1); hence, a chronic subcutaneous (Alzet) infusion method (delivering sVpr for 14 days) was adopted. Mean serum Vpr concentration in these sVpr-treated mice was 755 ± 16 pg/ml after 14 days (Fig. 1C).

### Whole-body lipolysis is increased in Vpr-Tg and sVpr-treated mice

Accelerated lipolysis is a cardinal metabolic defect in HIV patients (17–19). Lipid kinetic studies using steady-state infusions of isotopes of glycerol and palmitate (17) revealed that fasting total and net lipolysis were increased in Vpr-Tg mice of one line (Fig. 2A) (but not of another line; table S2) and in sVpr-treated mice (Fig. 2B). These Vpr-Tg and sVpr-treated mice had higher fasting respiratory exchange ratios (RERs) than their respective controls under the conditions of the infusion studies, indicating blunted fat oxidation (Fig. 2, C and D) for 4 hours early in the fasting period. However, longer calorimetry under conditions of chronic feeding with regular ($n$ = 11 wild type; $n$ = 10 Vpr-Tg) or high-fat ($n$ = 11 wild type; $n$ = 12 Vpr-Tg) diet, with the mice permitted to move freely, showed no group differences in fat oxidation averaged over 24 hours (table S3).

### Fat mass is diminished in Vpr-Tg and sVpr-treated mice

Although food intake was similar in Vpr-Tg and sVpr-treated mice compared to their respective controls (table S4), white adipose tissue (WAT) depots [inguinal fat (IF), perigonadal fat (PGF), and retroperitoneal fat (RPF)] were diminished in Vpr-Tg (Fig. 2E) and sVpr-treated mice (Fig. 2F). There were no group differences in brown adipose tissue mass.

### Expression of PPARγ target genes is blunted, whereas that of GR-regulated lipolytic genes is increased, in adipose tissues of Vpr-Tg and sVpr-treated mice

Accelerated lipolysis and diminished fat mass could result from PPARγ co-repression (14) or GR coactivation (12, 13) in adipose tissues. We quantified mRNA expression of PPARγ- and GR-regulated genes critical for fasting adipose metabolism. mRNA levels of the PPARγ targets *Pparγ* (Fig. 3A), *AdipoQ*, and *Ap2* (Fig. 3B) were diminished in IF of Vpr-Tg. Rosiglitazone did not affect the expression of *Pparγ* (Fig. 3A), *AdipoQ*, or *Ap2* (fig. S2) in either wild-type or Vpr-Tg IF. mRNA levels of PPARγ -regulated *Cap*, *Glut4*, *Cd36*, *Lpl*, and *Plin1* were also decreased in Vpr-Tg IF (Fig. 3B). Expression of *Atgl*, a GR-regulated gene responsible for triglyceride lipolysis, was increased, whereas that of *Hsl*, another GR-regulated gene that regulates diglyceride lipolysis, was decreased, in Vpr-Tg IF (Fig. 3C).

Similar results were noted in PGF, with some differences. mRNA levels of *Pparγ* (Fig. 3D), *AdipoQ*, and *Ap2* (Fig. 3E) were diminished in Vpr-Tg mice; rosiglitazone modestly increased *Pparγ* mRNA expression in wild-type but not in Vpr-Tg mice. Vpr's effect on the other PPARγ targets in PGF was more selective: mRNA levels of *Cap* were decreased, but those of *Glut4*, *Cd36*, *Lpl*, and *Plin1* were not different from wild type (Fig. 3E). mRNA expression of both *Atgl* and *Hsl* was increased in Vpr-Tg PGF (Fig. 3F).

To demonstrate that circulating Vpr can lead to adipose gene expression changes similar to those caused by Vpr expressed within adipose cells, we compared PPARγ and GR target gene mRNA levels in PGF of sVpr-treated and vehicle (water)–treated mice. Treatment with sVpr for 2 weeks decreased the mRNA levels of the PPARγ targets (Fig. 3G) and increased the mRNA levels of the GR-regulated lipolytic genes (Fig. 3H), similar to the changes observed in Vpr-Tg PGF.

## Plasma adiponectin and aP2 protein are diminished, and adipose levels of activated forms of lipolytic enzymes are increased, in Vpr-Tg

Plasma total and high–molecular weight (HMW) adiponectin protein were diminished in Vpr-Tg mice (Fig. 4, A and B). Rosiglitazone increased total and HMW adiponectin protein in both wild-type and Vpr-Tg mice. Plasma aP2 protein was also diminished in Vpr-Tg mice, with no effect of rosiglitazone (Fig. 4C).

Within IF, protein expression of adipose triglyceride lipase (ATGL) showed a trend ($P = 0.06$) to be increased in Vpr-Tg (Fig. 4D), congruent with increased *Atgl* mRNA. However, the ratio of phospho– hormone-sensitive lipase (HSL) ($Ser^{563}$) (indicating a β-adrenergic–regulated modification that activates catalytic activity) to total HSL was decreased in Vpr-Tg (Fig. 4D). Within PGF, ATGL protein was markedly increased in Vpr-Tg mice (Fig. 4E); furthermore, the ratio of phospho-HSL ($Ser^{563}$) to total HSL was increased in Vpr-Tg mice, whereas that of phospho-HSL ($Ser^{565}$) [indicating an adenosine monophosphate–activated protein kinase (AMPK)–regulated modification that does not activate lipolysis] to total HSL was not different (Fig. 4E). In sVpr-treated mice, as in Vpr-Tg mice, ATGL expression was elevated in both IF and PGF, whereas the ratio of phospho-HSL ($Ser^{563}$) to total HSL was decreased in IF but increased in PGF (Fig. 4F).

## Macrophage infiltration is increased and adipocytemorphology is altered in PGF of Vpr-Tg and sVpr-treated mice

Macrophage number was increased (Fig. 4, G and I) and adipocytes were larger (Fig. 4J) in PGF of Vpr-Tg mice. Macrophages, CLSs, and adipocyte size were also increased in PGF of sVpr-treated mice (Fig. 4, G, K, L, and M). Perilipin staining was diminished adjacent to CLSs, indicating increased adipocyte cell death in sVpr-treated mice (Fig. 4H).

## Vpr expressed in 3T3-L1 preadipocytes inhibits differentiation via cell cycle block, whereas Vpr expressed in mature adipocytes induces hyperlipolysis

To assess differential effects of Vpr on preadipocytes compared to mature adipocytes (both of which are present in adipose depots), we used a doxycycline-regulated lentiviral

expression system in 3T3-L1 cells, inducing either early (during preadipocyte proliferation) or late (after adipocyte differentiation) Vpr expression.

Vpr expression in proliferating preadipocytes completely blocked differentiation (Fig. 5A), associated with decreased expression of genes of the adipocyte development transcriptional cascade, from *Pref1/Dlk1* (early proliferation gene) through *Pparγ2* (early differentiation gene) to *Glut4* (late differentiation gene) (Fig. 5B). This early differentiation block (proximal to *Pparγ2* expression) in preadipocytes suggested a Vpr effect distinct from PPARγ co-repression. Flow cytometry revealed that Vpr expression induced cell cycle block at $G_2$-M; cell cycle arrest was attenuated, and preadipocyte differentiation gene expression and lipid accumulation were partially restored with expression of Vpr R80A, a mutant that blunts Vpr's cell cycle arrest function (Fig. 5C and fig. S3). Associated with the $G^2$-M block was a dysregulated increase in cyclin D1 expression (which normally occurs at the$G_1$-S transition) with some increase in cyclin B1 (Fig. 5D) and a sustained elevation of *Ccnd1* mRNA levels (encoding cyclin D1) (Fig. 5E) in the Vpr-expressing cells.

Vpr expression induced 48 hours after addition of differentiation medium did not block differentiation (fig. S4); however, β-adrenergic–stimulated lipolysiswas accelerated, as revealed by increased free fatty acid (FFA) release (Fig. 6, A and B) with a similar trend for glycerol release (Fig. 6, A and C).

These results indicated that whereas cell cycle arrest is a pathogenic mechanism in preadipocytes, the effects of Vpr in mature adipocytes involve different mechanisms, possibly PPARγ co-repression or GR co-activation. To test this, we performed chromatin immunoprecipitation (ChIP) assays in 3T3-L1 cells with lentivirus expression induced 72 hours after initiation of adipocyte differentiation, and quantified Vpr's effect on PPARγ-regulated (*AdipoQ* and *Ap2*) or GR-regulated (*Hsl*) gene expression. The levels of *AdipoQ* and *Ap2* promoter DNA immunoprecipitated by anti-PPARγ antibody after rosiglitazone treatment were lower in the Vpr compared to the control (rtTA) condition; in contrast, the level of *Hsl* promoter DNA immunoprecipitated by anti-GR antibody after dexamethasone treatment was higher in the Vpr condition (Fig. 6D).

## Expression of PPARα-regulated genes is down-regulated in liver of both Vpr mouse models

Because fat oxidation is blunted in HIV patients (17) and Vpr-exposed mice during the early fasting period, we quantified the mRNA expression of PPARα-regulated fat oxidation genes in liver of Vpr-Tg and wild-type littermates. mRNA levels of *Pparα* (Fig. 7A), *Cpt1α*, *Aox*, and *Lcad* (Fig. 7B) were decreased in Vpr-Tg. In liver of sVpr-treated mice, there was a decrease in *Lcad* mRNA and nonsignificant decreases in mRNA levels of the other oxidation genes (Fig. 7, C and D).

## Hepatosteatosis develops in both Vpr mouse models

HIV infection is associated with a high prevalence of hepatosteatosis (20). Hepatic fat was increased in Vpr-Tg (Fig. 7, F and G), with a 1.5-fold elevation of liver triglyceride content (Fig. 7E) and a modest increase in liver weight (Fig. 7H). Fat content and liver weight were

also increased in sVpr-treated mice after exposure to sVpr for only 2 weeks (Fig. 7, F, I, and J).

### Additional pathogenic pathways contribute to Vpr-induced hepatosteatosis

The rapid development of hepatosteatosis suggested pathogenic pathways in addition to increased FFA flux with impaired hepatic fat oxidation. Decreased plasma adiponectin levels in Vpr-Tg and sVpr-treated mice prompted investigation of its hepatic target AMPK (21), because decreased AMPK activity [resulting in lowered expression of PPARγ coactivator 1α (PGC1α) and thereby of PPARα (22, 23)] can cause hepatosteatosis (24). Activated ($Thr^{172}$-phosphorylated) AMPK relative to total AMPK was decreased in Vpr-Tg liver (Fig. 7K), as was *Pgc1α* mRNA (Fig. 7L). *Pepck* mRNA, whose expression in fasting liver is normally up-regulated by PGC1α (25), was also decreased in Vpr-Tg (Fig. 7L), explaining the low level of PEPCK promoter–driven Vpr transgene expression in liver compared to fat (Fig. 1B).

Intrahepatic apolipoprotein B–triglyceride packaging and transport are regulated by adipose differentiation–related protein (ADRP) [for very low density lipoprotein (VLDL)–triglyceride assembly and storage] and microsomal triglyceride transfer protein (MTP) (for VLDL-triglyceride export). PPARα positively regulates MTP transcription (26), and *Mtp* knockout induces fatty liver by inhibiting VLDL-triglyceride export (27). *Mtp* mRNA was diminished in Vpr-Tg liver (Fig. 7L).

### Vpr-Tg manifest hepatic insulin resistance and hyperglycemia

Hepatic insulin sensitivity, reflected by insulin-stimulated phospho-Akt ($Ser^{473}$), was diminished in Vpr-Tg (fig. S5A), associated with elevated postchallenge plasma glucose levels in young and older Vpr-Tg (fig. S5, B and C). Plasma insulin levels were not different (fig. S5D). Fasting plasma triglyceride levels were elevated in Vpr-Tg (fig. S5E), but FFA levels were not different (fig. S5F).

## DISCUSSION

Vpr circulates in the blood of HIV patients even after viral-suppressive treatment with ART, and its presence in the circulation of mice is sufficient to recapitulate the characteristic features of adipose and hepatic metabolic defects observed in HIV patients: accelerated lipolysis (17–19), diminished fat mass (7, 28), hepatosteatosis (20), insulin resistance, and hyperglycemia (29). Inhibition of PPAR-regulated signaling in fat and liver is a key mechanism in vivo because Vpr (i) represses PPARγ-regulated genes responsible for adipocyte differentiation, fatty acid transport, and insulin sensitization; (ii) represses PPARα-regulated genes of hepatic fat oxidation and VLDL-triglyceride export; and (iii) lowers adiponectin, leading to decreased liver AMPK-$Thr^{172}$ phosphorylation and diminished expression of Pgc1α. Concurrently, Vpr promotes the metabolic phenotype by coactivating GR-regulated genes in adipocytes (driving lipolysis) and via cell cycle arrest in preadipocytes (diminishing adipose mass).

Together with in vitro evidence for cellular- and nuclear-transducing activities of virion-free Vpr (16), these data demonstrate that Vpr drives mechanisms that may underlie the

metabolic defects in HIV patients. Vpr, produced by infected immune cells within reservoirs in HIV patients on ART (15), can transduce adipose tissues and liver to produce these metabolic defects (Fig. 8). Although the mouse models do not define the cells of origin of Vpr in natural HIV infection or latency, they support a pathogenic process whereby Vpr arriving at adipocytes or hepatocytes alters transcriptional regulation and function in those cells, and that Vpr can be transferred bidirectionally between these cells and the extracellular compartment in vivo. Furthermore, Vpr produced by HIV replicating in $CD4^+$ T cells can act in a paracrine manner on primary human subcutaneous adipocytes, altering mRNA expression of the PPARγ target *AdipoQ* and of the GR lipolysis-regulating targets *Atgl* and *Hsl* in a manner similar to that in IF of Vpr mice (fig. S6). Adverse effects of ART (4) could exacerbate lipodystrophic manifestations and contribute to heterogeneity in the clinical phenotype.

Gene expression studies of fat biopsies from HIV patients corroborate these results. Independent of ART, mRNA levels of PPARγ, adiponectin, and mitochondrial oxidative enzyme genes are reduced in subcutaneous adipose tissue of HIV patients (9). PPARγ positively regulates these genes, indicating that HIV-1 infection per se induces adipose defects via PPARγ repression, consistent with a Vpr effect. Similar gene expression defects occur in fat tissues of HIV-infected, untreated long-term nonprogressors (10) and in mice expressing a 7.7-kb HIV-1 construct (30).

Consistent with varying expression of adipokine genes in different human adipose depots (31) and regional differences in glucocorticoid sensitivity (32), repression of PPARγ-regulated genes was less, whereas activation of GR-regulated lipolytic genes (both *Atgl* and *Hsl*) was greater in PGF (analogous to human visceral fat) than in IF (analogous to human subcutaneous fat). In obese humans, lipolysis is higher in visceral than in subcutaneous fat (33), and the flux of fatty acids from this depot directly into the liver could drive hepatosteatosis.

GR signaling, which profoundly enhances ATGL expression (34), would increase ATGL activity and accelerate lipolysis in Vpr-Tg PGF. Protein kinase A activates HSL via $Ser^{563}$ phosphorylation, which was elevated in PGF but reduced in IF of Vpr-Tg mice. Glucocorticoids also up-regulate HSL expression (35). In mice, expression of ATGL [responsible for basal lipolysis (36)] is increased by fasting, whereas that of HSL is not. The coordinate increase in both ATGL protein and phospho-HSL ($Ser^{563}$) in PGF of Vpr mice is explained by enhanced glucocorticoid sensitization (12).

Adipose mass is regulated by turnover of preadipocytes through proliferation, differentiation, and apoptosis (37). Vpr expression in 3T3-L1 preadipocytes blocked differentiation, with down-regulation of genes of the relevant transcription factors. Cell cycle arrest at $G_2$-M, associated with continuously elevated expression of cyclin D1 [which interferes with PPARγ -mediated adipogenesis (38)], was a key mechanism of the differentiation block. Expression of the differentiation genes was not fully normalized by Vpr-R80A; hence, it is possible that mitochondria-dependent apoptosis by Vpr (39), which is also mitigated by the R80A mutation (40), contributes to the differentiation block. Expression of Vpr in differentiated adipocytes increased lipolysis and reciprocally altered

regulation of PPARγ and GR target genes involved in insulin sensitivity and lipolysis. Diminished WAT mass also occurred without increase in oxidative disposal of fat over 24 hours, indicating that accelerated lipolysis causes ectopic fat deposition in non-adipose organs, as is well described in HIV patients (41–43). Thus, multiple Vpr mechanisms produce lipoatrophy and hyperlipolysis.

Vpr increased macrophage number and CLSs in adipose tissue after exposure to circulating Vpr for only 2 weeks. Adipose tissue macrophages are derived from circulating monocytes; because FFAs are potent monocyte chemoattractants (44), Vpr-induced hyperlipolysis could directly promote macrophage accumulation in adipose depots.

Hepatosteatosis, which is highly prevalent in HIV patients, was induced by Vpr through pathways that likely include impaired fat oxidation (because of down-regulation of hepatic oxidative genes) in the face of increased FFA flux, and impaired clearance of VLDL-triglycerides (because of decreased Mtp expression). A common underlying mechanism is PPARα inhibition both directly by Vpr and indirectly through inhibition of adiponectin expression [leading to blunted hepatic AMPK activity (21) and thereby reduced expression (45) and transcriptional activation (23) of PGC1α (22, 23)]. Down-regulation of AMPK (24) or knockout of *Pgc1α* or *Mtp* (27) causes hepatosteatosis in mice.

Fasting hypertriglyceridemia, a hallmark of HIV-associated metabolic defects, was noted in Vpr-Tg mice in the present study [though not in our previous study of a different line of Vpr-Tg mice (46)], suggesting increased VLDL-triglyceride secretion despite diminished *Mtp* or a defect in VLDL-triglyceride clearance. Both increased secretion and decreased clearance of VLDL-triglycerides occur in HIV patients (18). Fasting plasma FFA levels were not elevated in Vpr-Tg mice, suggesting that increased adipocyte lipolysis is counterbalanced by increased hepatic extraction.

Serum levels of Vpr were not correlated with its quantitative effects on tissue gene or protein expression, lipid kinetics, or fat mass, suggesting a threshold level within the tissues and cells at which Vpr exerts its metabolic effects in tissues. This level cannot be determined from the present studies, but it is at or below that which was associated with the lowest serum Vpr levels in Vpr-Tg, and these are within the range of serum Vpr concentrations in HIV patients. Serum Vpr levels also were not correlated with HIV-1 VL; of note, serum levels of Nef, another HIV protein that is secreted from HIV-infected immune cells and has paracrine effects, are not correlated with HIV viremia (47).

The presence of Vpr in the circulation of optimally treated HIV patients and in adipose tissue and liver of HIV patients at autopsy provides translational relevance to these findings. The current data are limited in demonstrating the critical Vpr mechanisms in mice— full translation would require longitudinal metabolic measurements in blood and tissue specimens of HIV patients on cART with a range of serum Vpr levels and VL. In a cross-sectional analysis, we found no correlation between serum Vpr levels and lipid kinetic rates in 12 hyperlipolytic, hypertriglyceridemic HIV patients on cART with a range of VL, suggesting that Vpr has adipose-restricted effects not reflected quantitatively in serum Vpr concentrations. We infer that Vpr in the serum of patients reflects its production by HIV

sequestered in adipose tissue, liver, or other reservoirs but we have not measured Vpr production relative to HIV replication within those tissues or the kinetics of its extracellular transfer. Vpr is likely not the sole pathogenic factor in HIV-associated metabolic disturbances, but it has an independent effect. Confirmation of these mechanisms in patients could pave the way for targeted treatment with small-molecule inhibitors of Vpr, GR antagonists, or dual PPARγ /PPARα agonists.

## MATERIALS AND METHODS

### Study design

The study was designed to test the hypotheses that Vpr affects adipose and liver metabolism in mice and functions as a hormone in mice and HIV patients. Transgenic and pharmacologic mouse models were used to measure lipid kinetics and oxidation, quantitative expression of PPARγ and GR target gene transcripts and their protein products, ChIP, and insulin sensitivity. Hormonal characteristics were determined by measuring serum Vpr levels in mice and stored samples of HIV patients. Sample sizes for all mouse experiments were based on previous experience with Vpr transgenic mice (46). Statistical analyses are described below. Investigators were blinded to all mouse and HIV-infected human sera used for Vpr measurements, and to liver samples used for immunohistochemistry and Oil Red O quantification.

### Vpr-Tg mice

Protocols were approved by the Baylor Institutional Animal Care and Use Committee. Vpr-Tg mice expressing PEPCK promoter–driven Vpr under the control of a tetracycline-repressible (tTA) system were constructed at the National Institutes of Health (NIH) (46). Two transgenic lines were rederived at Baylor. Fourteen- to 16-week-old male mice were used in all experiments.

### Synthetic Vpr

sVpr was produced by solid-state peptide synthesis, purified, characterized by sequencing and mass spectrometry (MS), and compared to viral Vpr by SDS–polyacrylamide gel electrophoresis (PAGE) and immunoblot (48). The stability of the peptide in aqueous solution was confirmed by dynamic light scattering, circular dichroism, and $^{1}H$ nuclear magnetic resonance spectroscopy (48).

### sVpr infusions

Alzet pumps (model 1002, Durect), containing aqueous solution of sVpr or sterile water, were implanted subcutaneously in wild-type mice with delivery rate of 0.25 μl/hour to administer 5 μg of sVpr every 24 hours for 14 days.

### Serum Vpr

Serum Vpr was measured in coded samples using ICE (46). This electrokinetic assay uses immobilized monoclonal antibodies (mAbs) to isolate Vpr before separation and online detection by laser-induced fluorescence in samples ≥1 μl. Detection limits were determined

using mouse serum standards "spiked" with sVpr. Liquid chromatography– MS and matrix-assisted laser desorption/ionization analysis confirmed that the recovered analyte was comparable to the Vpr used to raise the anti-Vpr antibody for ICE. The specificity of the capture antibody was tested using two-dimensional electrophoresis blots of Vpr, HIV surface and internal antigens, and T cell receptors. The antibody demonstrated reactivity only against Vpr. The sensitivity of the assay was in the range of 1.5 to 2100 pg/ml. Intra- and interassay coefficients of variation were 3.22 and 4.13%, respectively.

### Lipid kinetics

Lipid kinetics were measured in Vpr-Tg or wild-type littermates and in wild-type mice receiving sVpr or water (in the latter, 13 days after Alzet placement). Calorimetry (Columbus Instruments) was performed before the kinetic study to measure $VO_2$ and $VCO_2$ under the same conditions as for the isotope infusions (for 4 hours after onset of fasting). The next day, mice received primed (P)–constant IV (I) infusions of [$^{13}C_1$] palmitate (P = 75 μmol/kg, I = 75 μmol/kg per hour) and [$^2H_5$]glycerol (P = 140 μmol/kg, I = 140 μmol/kg per hour) for 4 hours. Blood was collected in prechilled $Na_2$EDTA tubes and centrifuged at 4°C, and the plasma was stored at −80°C.

Plasma palmitate isotope ratio was determined on the pentafluorobenzyl derivative by negative chemical ionization–GC/MS, with selective ion monitoring at mass/charge ratio (*m/z*) 255 and 256 (Hewlett-Packard); glycerol isotope ratio was measured on the glycerol tripropylester derivative by electron impact–GC/MS, with ion monitoring at *m/z* 173 to 176. Standard steady-state equations were used to calculate fluxes of palmitate and glycerol; these, with the concentration ratio of plasma palmitate (determined by isotope dilution using [$^2H_2$] palmitate) to FFA (Wako), were used to calculate total and net lipolysis (17). Respiratory exchange ratio (RER = $VO_2/VCO_2$) provided an index of the fuel substrate oxidized.

Twenty-four–hour calorimetry was also performed in wild-type mice and Vpr-Tg under conditions of chronic feeding with regular chow or high-fat (60%) diet.

### Effects of Vpr on adipose tissue and liver

Vpr-Tg and wild-type littermates were placed on high-protein diet (Harlan-Teklad) for 3 weeks to activate the PEPCK/tTA promoter. Subgroups of mice were treated with rosiglitazone (10 mg/kg per day, intraperitoneally) or vehicle for 14 days (dose and duration optimized for adipose expression of *Pparγ* and *Glut4* mRNA). Mice were fasted for 15 hours and euthanized in the morning. Blood and tissues were collected, and plasma was immediately separated. Tissues were snap-frozen for RNA and protein extraction and stored at −80°C or fixed in 10% formalin for immunohistochemistry.

### mRNA levels

Total RNA was extracted from liver using TRIzol (Invitrogen) and from adipose tissue using a lipid extraction kit (Qiagen) and transcribed using the RNA-to-cDNA kit (Applied Biosystems), and polymerase chain reaction (PCR) was performed with the TaqMan assay. PPARγ/GR target genes included, in adipose tissues, adiponectin (*AdipoQ*), adipocyte

protein 2 (*aP2*), Cbl-associated protein (*Cap*), *Glut4*, *Cd36*, perilipin (*Plin1*), adipocyte triglyceride lipase (*Atgl*), and hormone-sensitive lipase (*Hsl*); in liver, carnitine palmitoyl transferase-1a (Cpt1α), acyl coenzyme A (CoA) oxidase (*Aox*), long-chain acyl CoA dehydrogenase (*Lcad*), uncoupling protein-2 (*Ucp2*), and microsomal triglyceride transfer protein (*Mtp*). *Pgk1* mRNA was used for normalization.

### Enzyme-linked immunosorbent assay

Plasma concentrations of adiponectin (BioVendor) and aP2 (Invitrogen) were measured by enzyme-linked immunosorbent assay following the manufacturers' protocols.

### Immunoblotting

After extraction in radioimmunoprecipitation assay (RIPA) with phosphatase and protease inhibitors, proteins were resolved by SDS-PAGE and identified after transfer by ECL (Thermo Fisher). Primary antibodies for AMPK, phospho-AMPK ($Thr^{172}$), Akt, phospho-Akt ($Ser^{473}$), ATGL, HSL, phospho-HSL ($Ser^{563}$), and phospho-HSL ($Ser^{565}$) were from Cell Signaling. Immunoblots were scanned, and densitometry was quantified using ImageJ software.

### Thin-layer chromatography

Lipids were extracted from 0.2 g of liver, dried under nitrogen, reconstituted in chloroform, and loaded onto a thin-layer chromatography (TLC) plate with standards to identify lipid species. Lipid fractions were visualized using iodine vapor. TLC plates were scanned, and lipid species were quantified by densitometry using ImageJ software.

### Oil Red O staining

Cryostat sections of liver were cut, fixed in 10% formalin, and stained with Oil Red O. For each section, three to four pictures of different fields were taken at ×20 magnification. Staining was quantified using ImageJ software.

### Adipose tissue histomorphometry/immunohistochemistry

Sections were stained for expression of F4/80 and perilipin (Abcam) using standard protocols, and pictures of different fields were taken at ×10 to ×20 magnification (three mice per group). Adipocytes were counted in two sections per mouse at ×10 magnification by observers masked to the treatment. $F4/80^{+}$ nuclei were counted in nine sections per group. Average cell size was calculated by dividing section area by cell number.

### Vpr effects on adipocyte differentiation and function

Vpr complementary DNA (cDNA) was cloned into a tetracycline-inducible lentivirus system (gift of R. Schwartz, University of Houston) with tet-responsive promoter elements (TREs) driving transgene expression and a second lentivirus vector encoding the doxycycline-activated reverse tetracycline transactivator (rtTA). Standard methods were used for virus packaging and propagation. Vector particles were concentrated by ultracentrifugation and titered using Retro-X Kits (Clontech). 3T3-L1 cells and their media for growth, induction, and differentiation were from ZenBio. 3T3-L1 preadipocytes (70%

confluence) were infected with lentivirus constructs (TRE-Vpr or TRE and rtTA). For early Vpr expression experiments (Vpr effects in preadipocytes), doxycycline (1 μg/ml) was added 48 hours later (day 0). Differentiation medium (containing insulin, dexamethasone, and PPARγ agonist) was added 48 hours later (day 2) followed by adipocyte maintenance medium. Cells were harvested daily (days 1 to 10), and RNA was isolated (Qiagen). For late Vpr expression experiments (Vpr effects in mature adipocytes), differentiation medium was added on day 2, doxycycline was added to induce transgene expression on day 4, and cells were harvested on day 5 [for quantitative reverse transcription PCR (qRT-PCR) and ChIP] or day 6 (for lipolysis). For qRT-PCR, first-strand cDNA synthesis from total RNA was performed with Superscript III First-Strand Synthesis Kit with oligo(dT) (Invitrogen). qPCR was performed with SYBR Green PCR mix in a Stratagene MX 3000P machine. Levels of *Pref1/Glk1*, *Pparγ2*, *Ap2*, and *Glut4* mRNA were measured using validated probes (http://pga.mgh.harvard.edu/primerbank/). Lipolysis was measured on day 6 according to the manufacturer's instructions (ZenBio). Cells were treated in quadruplicate with phosphate-buffered saline (PBS) or CL316243 ($\beta_3$-adrenoceptor agonist) for 3 hours. Glycerol and FFA concentrations were measured in the supernatants using a kit(Wako). For ChIP to assay Vpr effect on PPARγ- or GR-regulated adipocyte genes, on day 5, cells were treated with DMSO (vehicle), 1 μM rosiglitazone, or 10 nM dexamethasone for 24 hours and formaldehyde, and ChIP was performed according to the Abcam protocol (http://www.abcam.com/ps/pdf/protocols/x_CHip_protocol.pdf). Immunoprecipitation antibodies were directed against PPARγ (Abcam) or GR (Cell Signaling), with rabbit immunoglobulin G (Abcam) as control. Promoter-targeting primer sequences for qPCR are reported in table S5. For negative controls, primers targeting off-target sites ~2 kb upstream of the respective target peroxisome proliferator gamma response element (PPRE) or glucocorticoid response element (GRE) were used.

### Flow cytometry of cell cycle and cyclin expression

3T3-L1 cells were stained with propidium iodide (PI) and cyclin mAbs. Cells ($5 \times 10^5$) were trypsinized, washed with PBS, fixed with 4 ml of 100% methanol at 4°C overnight, permeabilized in 1 ml of PBS/0.25% Triton on ice for 5 min, washed with PBS/2% fetal bovine serum (FBS), and incubated with mAbs or isotype controls (1 μg/ml) for 1 hour at 4°C. Cells were washed with PBS/2% FBS and incubated with PI (50 μg/ml) (Sigma) and ribonuclease (100 μg/ml) (Sigma) for 1 hour at 4°C. Data were acquired on a Gallios flow cytometer and analyzed with Kaluza 1.2 software (Beckman-Coulter).

Plasma triglyceride levels were measured using the GPO Trinder reagent (Thermo Scientific).

### Human subjects

Serum samples for Vpr measurement were collected from HIV-negative subjects and HIV patients on cART who gave informed consent under clinical research protocols approved by the Baylor and National Institute of Diabetes and Digestive and Kidney Diseases (NIDDK) Institutional Review Boards. Sera from ART-naïve and NRTI-treated HIV patients were obtained from deidentified stored samples of participants previously enrolled in an Institutional Review Board–approved vaccine trial.

### Statistics

One-way analysis of variance (ANOVA) with Bonferroni's multiple comparison test was used for analysis of serum Vpr levels in HIV-infected patients. All animal experiments involved two-way comparisons between wild-type and experimental conditions; hence, two-tailed, unpaired *t* tests for unequal variance were used. For lentiviral studies involving comparisons between uninfected control, rtTA control, and the other experimental conditions, or wild-type Vpr compared to Vpr-R80A at different time points, two-way ANOVA with Bonferroni's multiple comparison test was applied. Data are presented as means ± SE. $P < 0.05$ was considered significant.

## Supplementary Material

Refer to Web version on PubMed Central for supplementary material.

## Acknowledgments

We thank H. Mersmann, L. A. Cowart, V. Yechoor, B. Chang, and H. J. Pownall for valuable discussions; J. W. Hsu, S. Hartig, P. Saha, and W. Chen for experimental help; and E. Davidson and D. Nguyen for technical assistance. We are grateful to the late P. J. Reeds for insights that guided this study. **Funding**: This work was supported by DK081553 and a Developmental Grant from the Baylor Center for AIDS Research P30AI36211 (to A.B.), a Seed award (to R.V.S.), P30DK079638 (Diabetes Research Center at Baylor), German Research Council grants SFB 796 and 643 (to U.S.), the NIDDK Intramural Research Program, and the NIH Office of the Director.

## REFERENCES AND NOTES

1. Lyons MJ, Faust IM, Hemmes RB, Buskirk DR, Hirsch J, Zabriskie JB. A virally induced obesity syndrome in mice. Science. 1982; 216:82–85. [PubMed: 7038878]
2. Ramesh S, Sanyal AJ. Hepatitis C and nonalcoholic fatty liver disease. Semin. Liver Dis. 2004; 24:399–413. [PubMed: 15605308]
3. Dhurandhar NV. A framework for identification of infections that contribute to human obesity. Lancet Infect. Dis. 2011; 11:963–969. [PubMed: 22115071]
4. Carr A, Miller J, Law M, Cooper DA. A syndrome of lipoatrophy, lactic acidaemia and liver dysfunction associated with HIV nucleoside analogue therapy: Contribution to protease inhibitor-related lipodystrophy syndrome. AIDS. 2000; 14:F25–F32. [PubMed: 10716495]
5. Pond CM. Long-term changes in adipose tissue in human disease. Proc. Nutr. Soc. 2001; 60:365–374. [PubMed: 11681811]
6. Grunfeld C, Kotler DP, Hamadeh R, Tierney A, Wang J, Pierson RN. Hypertriglyceridemia in the acquired immunodeficiency syndrome. Am. J. Med. 1989; 86:27–31. [PubMed: 2910092]
7. Visnegarwala F, Raghavan SS, Mullin CM, Bartsch G, Wang J, Kotler D, Gibert CL, Shlay J, Grunfeld C, Carr A, El-Sadr W. Sex differences in the associations of HIV disease characteristics and body composition in antiretroviral-naive persons. Am. J. Clin. Nutr. 2005; 82:850–856. [PubMed: 16210716]
8. Madge S, Kinloch-de-Loes S, Mercey D, Johnson MA, Weller IV. Lipodystrophy in patients naive to HIV protease inhibitors. AIDS. 1999; 13:735–737. [PubMed: 10397574]
9. Giralt M, Domingo P, Guallar JP, Rodriguez de la Concepción ML, Alegre M, Domingo JC, Villarroya F. HIV-1 infection alters gene expression in adipose tissue, which contributes to HIV- 1/HAART-associated lipodystrophy. Antivir. Ther. 2006; 11:729–740. [PubMed: 17310817]
10. Vidal F, Domingo P, Villarroya F, Giralt M, López-Dupla M, Gutiérrez M, Gallego-Escuredo JM, Peraire J, Viladés C, Veloso S, Mateo G, Guallar JP, Richart C. Adipogenic/lipid, inflammatory, and mitochondrial parameters in subcutaneous adipose tissue of untreated HIV-1-infected long-term nonprogressors: Significant alterations despite low viral burden. J. Acquir. Immune Defic. Syndr. 2012; 61:131–137. [PubMed: 22580565]

11. Kino T, Chrousos GP. Human immunodeficiency virus type-1 accessory protein Vpr: A causative agent of the AIDS-related insulin resistance/lipodystrophy syndrome? Ann. N. Y. Acad. Sci. 2004; 1024:153–167. [PubMed: 15265780]
12. Kino T, Gragerov A, Kopp JB, Stauber RH, Pavlakis GN, Chrousos GP. The HIV-1 virion-associated protein Vpr is a coactivator of the human glucocorticoid receptor. J. Exp. Med. 1999; 189:51–62. [PubMed: 9874563]
13. Kino T, Gragerov A, Slobodskaya O, Tsopanomichalou M, Chrousos GP, Pavlakis GN. Human immunodeficiency virus type 1 (HIV-1) accessory protein Vpr induces transcription of the HIV-1 and glucocorticoid-responsive promoters by binding directly to p300/CBP coactivators. J. Virol. 2002; 76:9724–9734. [PubMed: 12208951]
14. Shrivastav S, Kino T, Cunningham T, Ichijo T, Schubert U, Heinklein P, Chrousos GP, Kopp JB. Human immunodeficiency virus (HIV)-1 viral protein R suppresses transcriptional activity of peroxisome proliferator-activated receptor γ and inhibits adipocyte differentiation: Implications for HIV-associated lipodystrophy. Mol. Endocrinol. 2008; 22:234–247. [PubMed: 17932108]
15. Poon B, Grovit-Ferbas K, Stewart SA, Chen IS. Cell cycle arrest by Vpr in HIV-1 virions and insensitivity to antiretroviral agents. Science. 1998; 281:266–269. [PubMed: 9657723]
16. Sherman MP, Schubert U, Williams SA, de Noronha CM, Kreisberg JF, Henklein P, Greene WC. HIV-1 Vpr displays natural protein-transducing properties: Implications for viral pathogenesis. Virology. 2002; 302:95–105. [PubMed: 12429519]
17. Sekhar RV, Jahoor F, White AC, Pownall HJ, Visnegarwala F, Rodriguez-Barradas MC, Sharma M, Reeds PJ, Balasubramanyam A. Metabolic basis of HIV-lipodystrophy syndrome. Am. J. Physiol. Endocrinol. Metab. 2002; 283:E332–E337. [PubMed: 12110539]
18. Reeds DN, Mittendorfer B, Patterson BW, Powderly WG, Yarasheski KE, Klein S. Alterations in lipid kinetics in men with HIV-dyslipidemia. Am. J. Physiol. Endocrinol. Metab. 2003; 285:E490–E497. [PubMed: 12746213]
19. Hadigan C, Borgonha S, Rabe J, Young V, Grinspoon S. Increased rates of lipolysis among human immunodeficiency virus–infected men receiving highly active antiretroviral therapy. Metabolism. 2002; 51:1143–1147. [PubMed: 12200758]
20. Li Vecchi V, Soresi M, Giannitrapani L, Di Carlo P, Mazzola G, Colletti P, Terranova A, Vizzini G, Montalto G. Prospective evaluation of hepatic steatosis in HIV-infected patients with or without hepatitis C virus co-infection. Int. J. Infect. Dis. 2012; 16:e397–e402. [PubMed: 22425495]
21. Yamauchi T, Kamon J, Minokoshi Y, Ito Y, Waki H, Uchida S, Yamashita S, Noda M, Kita S, Ueki K, Eto K, Akanuma Y, Froguel P, Foufelle F, Ferre P, Carling D, Kimura S, Nagai R, Kahn BB, Kadowaki T. Adiponectin stimulates glucose utilization and fatty-acid oxidation by activating AMP-activated protein kinase. Nat. Med. 2002; 8:1288–1295. [PubMed: 12368907]
22. Vega RB, Huss JM, Kelly DP. The coactivator PGC-1 cooperates with peroxisome proliferator-activated receptor α in transcriptional control of nuclear genes encoding mitochondrial fatty acid oxidation enzymes. Mol. Cell. Biol. 2000; 20:1868–1876. [PubMed: 10669761]
23. Jäger S, Handschin C, St-Pierre J, Spiegelman BM. AMP-activated protein kinase (AMPK) action in skeletal muscle via direct phosphorylation of PGC-1α. Proc. Natl. Acad. Sci. U.S.A. 2007; 104:12017–12022. [PubMed: 17609368]
24. Browning JD, Horton JD. Molecular mediators of hepatic steatosis and liver injury. J. Clin. Invest. 2004; 114:147–152. [PubMed: 15254578]
25. Koo SH, Satoh H, Herzig S, Lee CH, Hedrick S, Kulkarni R, Evans RM, Olefsky J, Montminy M. PGC-1 promotes insulin resistance in liver through PPAR-a-dependent induction of TRB-3. Nat. Med. 2004; 10:530–534. [PubMed: 15107844]
26. Améen C, Edvardsson U, Ljungberg A, Asp L, Akerblad P, Tuneld A, Olofsson SO, Lindén D, Oscarsson J. Activation of peroxisome proliferator-activated receptor α increases the expression and activity of microsomal triglyceride transfer protein in the liver. J. Biol. Chem. 2005; 280:1224–1229. [PubMed: 15537571]
27. Raabe M, Véniant MM, Sullivan MA, Zlot CH, Björkegren J, Nielsen LB, Wong JS, Hamilton RL, Young SG. Analysis of the role of microsomal triglyceride transfer protein in the liver of tissue-specific knockout mice. J. Clin. Invest. 1999; 103:1287–1298. [PubMed: 10225972]

28. Bacchetti P, Gripshover B, Grunfeld C, Heymsfield S, McCreath H, Osmond D, Saag M, Scherzer R, Shlipak M, Tien P. Study of Fat Redistribution and Metabolic Change in HIV Infection (FRAM), Fat distribution in men with HIV infection. J. Acquir. Immune Defic. Syndr. 2005; 40:121–131. [PubMed: 16186728]
29. Dubé MP. Disorders of glucose metabolism in patients infected with human immunodeficiency virus. Clin. Infect. Dis. 2000; 31:1467–1475. [PubMed: 11096014]
30. Villarroya J, Diaz-Delfin J, Hyink D, Domingo P, Giralt M, Klotman PE, Villarroya F. HIV type-1 transgene expression in mice alters adipose tissue and adipokine levels: Towards a rodent model of HIV type-1 lipodystrophy. Antivir. Ther. 2010; 15:1021–1028. [PubMed: 21041917]
31. Montague CT, Prins JB, Sanders L, Zhang J, Sewter CP, Digby J, Byrne CD, O'Rahilly S. Depot-related gene expression in human subcutaneous and omental adipocytes. Diabetes. 1998; 47:1384–1391. [PubMed: 9726225]
32. Rebuffé-Scrive M, Lundholm K, Björntorp P. Glucocorticoid hormone binding to human adipose tissue. Eur. J. Clin. Invest. 1985; 15:267–271. [PubMed: 3935457]
33. Arner P. Differences in lipolysis between human subcutaneous and omental adipose tissues. Ann. Med. 1995; 27:435–438. [PubMed: 8519504]
34. Villena JA, Roy S, Sarkadi-Nagy E, Kim KH, Sul HS. Desnutrin, an adipocyte gene encoding a novel patatin domain-containing protein, is induced by fasting and glucocorticoids: Ectopic expression of desnutrin increases triglyceride hydrolysis. J. Biol. Chem. 2004; 279:47066–47075. [PubMed: 15337759]
35. Yu CY, Mayba O, Lee JV, Tran J, Harris C, Speed TP, Wang JC. Genome-wide analysis of glucocorticoid receptor binding regions in adipocytes reveal gene network involved in triglyceride homeostasis. PLoS One. 2010; 5:e15188. [PubMed: 21187916]
36. Zechner R, Kienesberger PC, Haemmerle G, Zimmermann R, Lass A. Adipose triglyceride lipase and the lipolytic catabolism of cellular fat stores. J. Lipid Res. 2009; 50:3–21. [PubMed: 18952573]
37. Gregoire FM, Smas CM, Sul HS. Understanding adipocyte differentiation. Physiol. Rev. 1998; 78:783–809. [PubMed: 9674695]
38. Fu M, Rao M, Bouras T, Wang C, Wu K, Zhang X, Li Z, Yao TP, Pestell RG. Cyclin D1 inhibits peroxisome proliferator-activated receptor γ-mediated adipogenesis through histone deacetylase recruitment. J. Biol. Chem. 2005; 280:16934–16941. [PubMed: 15713663]
39. Muthumani K, Hwang DS, Desai BM, Zhang D, Dayes N, Green DR, Weiner DB. HIV-1Vpr induces apoptosis through caspase 9 in T cells and peripheral blood mononuclear cells. J. Biol. Chem. 2002; 277:37820–37831. [PubMed: 12095993]
40. Andersen JL, DeHart JL, Zimmerman ES, Ardon O, Kim B, Jacquot G, Benichou S, Planelles V. HIV-1 Vpr-induced apoptosis is cell cycle dependent and requires Bax but not ANT. PLoS Pathog. 2006; 2:e127. [PubMed: 17140287]
41. Sutinen J, Häkkinen AM, Westerbacka J, Seppälä-Lindroos A, Vehkavaara S, Halavaara J, Järvinen A, Ristola M, Yki-Järvinen H. Increased fat accumulation in the liver in HIV-infected patients with antiretroviral therapy-associated lipodystrophy. AIDS. 2002; 16:2183–2193. [PubMed: 12409740]
42. Gan SK, Samaras K, Thompson CH, Kraegen EW, Carr A, Cooper DA, Chisholm DJ. Altered myocellular and abdominal fat partitioning predict disturbance in insulin action in HIV protease inhibitor-related lipodystrophy. Diabetes. 2002; 51:3163–3169. [PubMed: 12401706]
43. Orlando G, Guaraldi G, Zona S, Carli F, Bagni P, Menozzi M, Cocchi S, Scaglioni R, Ligabue G, Raggi P. Ectopic fat is linked to prior cardiovascular events in men with HIV. J. Acquir. Immune Defic. Syndr. 2012; 59:494–497. [PubMed: 22410868]
44. Kosteli A, Sugaru E, Haemmerle G, Martin JF, Lei J, Zechner R, Ferrante AW Jr. Weight loss and lipolysis promote a dynamic immune response in murine adipose tissue. J. Clin. Invest. 2010; 120:3466–3479. [PubMed: 20877011]
45. Jørgensen SB, Wojtaszewski JF, Viollet B, Andreelli F, Birk JB, Hellsten Y, Schjerling P, Vaulont S, Neufer PD, Richter EA, Pilegaard H. Effects of α-AMPK knockout on exercise-induced gene activation in mouse skeletal muscle. FASEB J. 2005; 19:1146–1148. [PubMed: 15878932]

46. Balasubramanyam A, Mersmann H, Jahoor F, Phillips TM, Sekhar RV, Schubert U, Brar B, Iyer D, Smith EO, Takahashi H, Lu H, Anderson P, Kino T, Henklein P, Kopp JB. Effects of transgenic expression of HIV-1 Vpr on lipid and energy metabolism in mice. Am. J. Physiol. Endocrinol. Metab. 2007; 292:E40–E48. [PubMed: 16882932]

47. Raymond AD, Campbell-Sims TC, Khan M, Lang M, Huang MB, Bond VC, Powell MD. HIV type 1 Nef is released from infected cells in $CD45^+$ microvesicles and is present in the plasma of HIV-infected individuals. AIDS Res. Hum. Retroviruses. 2011; 27:167–178. [PubMed: 20964480]

48. Henklein P, Bruns K, Sherman MP, Tessmer U, Licha K, Kopp J, de Noronha CM, Greene WC, Wray V, Schubert U. Functional and structural characterization of synthetic HIV-1 Vpr that transduces cells, localizes to the nucleus, and induces $G_2$ cell cycle arrest. J. Biol. Chem. 2000; 275:32016–32026. [PubMed: 10903315]

49. Mödder UI, Monroe DG, Fraser DG, Spelsberg TC, Rosen CJ, Géhin M, Chambon P, O'Malley BW, Khosla S. Skeletal consequences of deletion of steroid receptor coactivator-2/transcription intermediary factor-2. J. Biol. Chem. 2009; 284:18767–18777. [PubMed: 19423703]

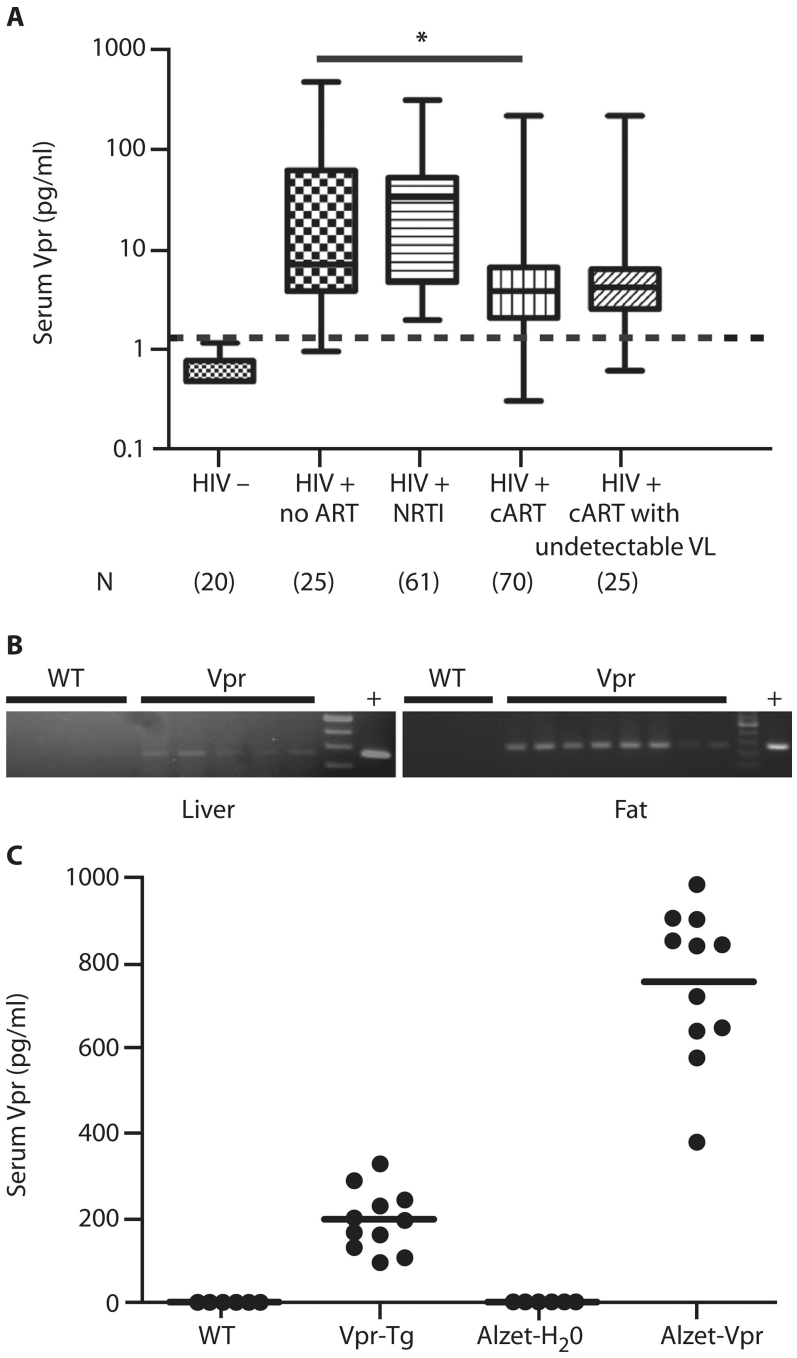


**Fig. 1. Vpr in HIV patients and mouse models**

(**A**) Box-and-whisker plots of serum Vpr concentrations in HIV-negative persons and four HIV-infected groups: ART-naïve, on NRTI only, on cART, and on cART with undetectable VL. Median Vpr concentrations in patients: ART-naïve = 7.0 pg/ml; NRTI only = 32.0 pg/ml; cART = 3.9 pg/ml; cART with undetectable VL = 4.2 pg/ml. Whiskers indicate minimum and maximum of all data. Dashed line indicates cutoff between false- and true-positive values. False-positive rate = 3% ART-naïve HIV, 0% HIV on NRTI, 6% HIV on cART, and 4% HIV on cART with undetectable VL. (**B**) Vpr mRNA in liver of Vpr-Tg (*n* = 5) compared to wild-type (WT) littermates (*n* = 5) and in PGF of Vpr-Tg (*n* = 8) compared to WT (*n* = 5); “+” indicates

positive control DNA. (**C**) Vpr protein in sera of Vpr-Tg and sVpr-treated mice. Horizontal lines indicate mean values. *$P$ = 0.001 for ART-naïve compared to cART-treated HIV patients.

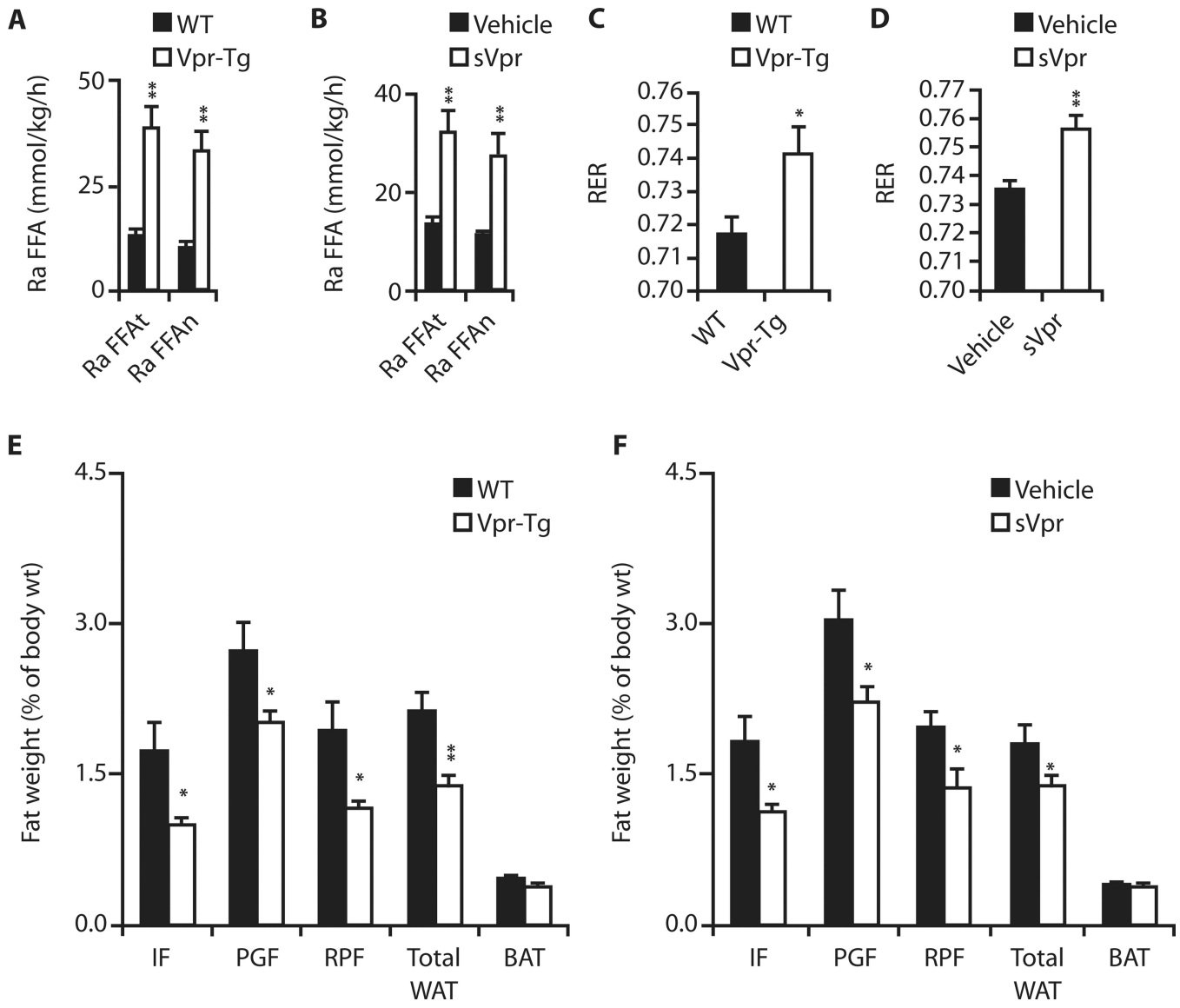


**Fig. 2. Altered fasting lipid kinetics and fat mass in Vpr-Tg and sVpr-treated mice**

(**A** and **B**) Accelerated fasting total and net lipolysis in (A) Vpr-Tg ($n$ = 6 per group; $P$ = 0.007 and 0.005) and (B) sVpr-treated ($n$ = 7) compared to water (vehicle)–treated ($n$ = 4) mice ($P$ = 0.01 and 0.006). Ra FFAt, total free fatty acid plasma entry rate (total lipolysis); Ra FFAn, net free fatty acid plasma entry rate (net lipolysis). (**C** and **D**) Increased RER during initial 4 hours of fasting in (C) Vpr-Tg ($n$ = 5 per group; $P$ = 0.04) and (D) sVpr-treated ($n$ = 5 per group; $P$ = 0.005) mice. (**E**) Reduced IF ($P$ = 0.03), PGF ($P$ = 0.05), RPF ($P$ = 0.05), and total WAT ($P$ = 0.001) mass (normalized to body weight) in Vpr-Tg ($n$ = 8 per group) mice. (**F**) Reduced IF ($P$ = 0.03), PGF ($P$ = 0.03), RPF ($P$ = 0.04), and total WAT ($P$ = 0.03) mass in sVpr-treated ($n$ = 8 per group) mice. BAT, brown adipose tissue. Values are means ± SE. *$P$ < 0.05, **$P$ < 0.01.

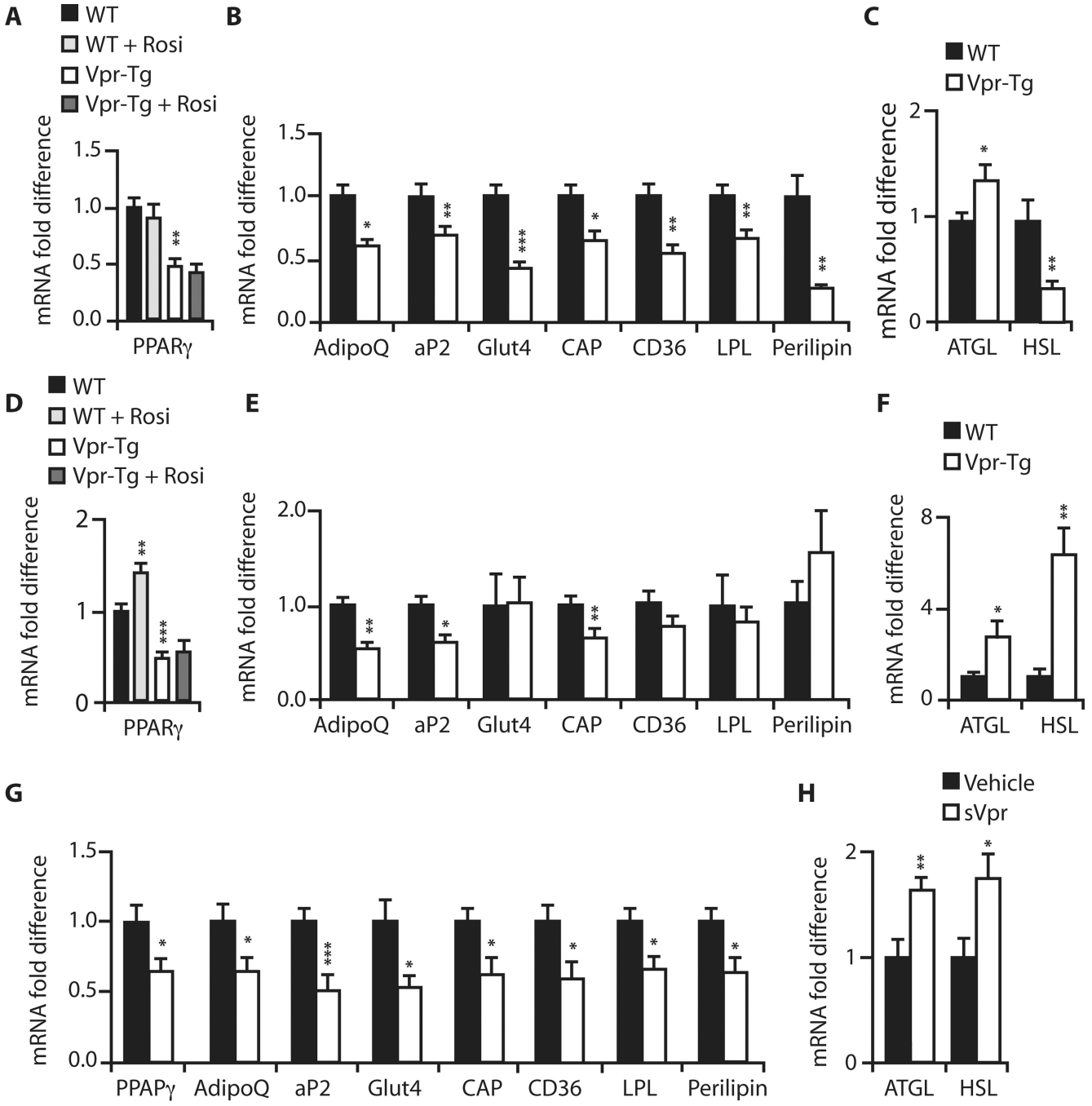


**Fig. 3. Altered expression of PPARγ- and GR-regulated genes in PGF and IF of Vpr-Tg and PGF of sVpr-treated mice**

(**A**) Reduced *Pparγ* mRNA in IF of Vpr-Tg ($P = 0.01$); rosiglitazone had no effect. (**B**) Reduced *AdipoQ* ($P = 0.02$), *Ap2* ($P = 0.009$), *Glut4* ($P = 0.0003$), *Cap* ($P = 0.03$), *Cd36* ($P = 0.005$), *Lpl* ($P = 0.01$), and *Plin1* ($P = 0.003$) mRNA in IF of Vpr-Tg. (**C**) Increased *Atgl* ($P = 0.04$) and reduced *Hsl* ($P = 0.01$) mRNA in IF of Vpr-Tg. (**D**) Reduced *Pparγ* mRNA in PGF of Vpr-Tg ($P = 0.001$); rosiglitazone increased mRNA expression in WT ($P = 0.01$) but not in Vpr-Tg. (**E**) Reduced *AdipoQ* ($P = 0.01$), *Ap2* ($P = 0.03$), *Cap* ($P = 0.01$), *Glut4* ($P = 0.95$), *Cd36* ($P = 0.22$), *Lpl* ($P = 0.90$), and *Plin1* ($P = 0.30$) mRNA in PGF of Vpr-Tg. (**F**) Increased *Atgl* ($P = 0.05$) and *Hsl* ($P = 0.002$) mRNA in PGF of Vpr-Tg. (**G**) ReducedmRNA of *Pparγ* ($P = 0.03$), *AdipoQ* ($P = 0.04$), *Ap2* ($P = 0.001$), *Glut4* ($P = 0.02$), *Cap* ($P = 0.02$), *Cd36* ($P = 0.02$), *Lpl* ($P = 0.02$), and *Plin1* ($P = 0.02$) in

PGF of sVpr-treated mice. (**H**) Increased *Atgl* ($P = 0.01$) and *Hsl* ($P = 0.02$) mRNA in PGF of sVpr-treated mice. $n = 8$ per group for all experiments. Values are means ± SE. $^{*}P < 0.05$, $^{**}P < 0.01$, $^{***}P < 0.001$.

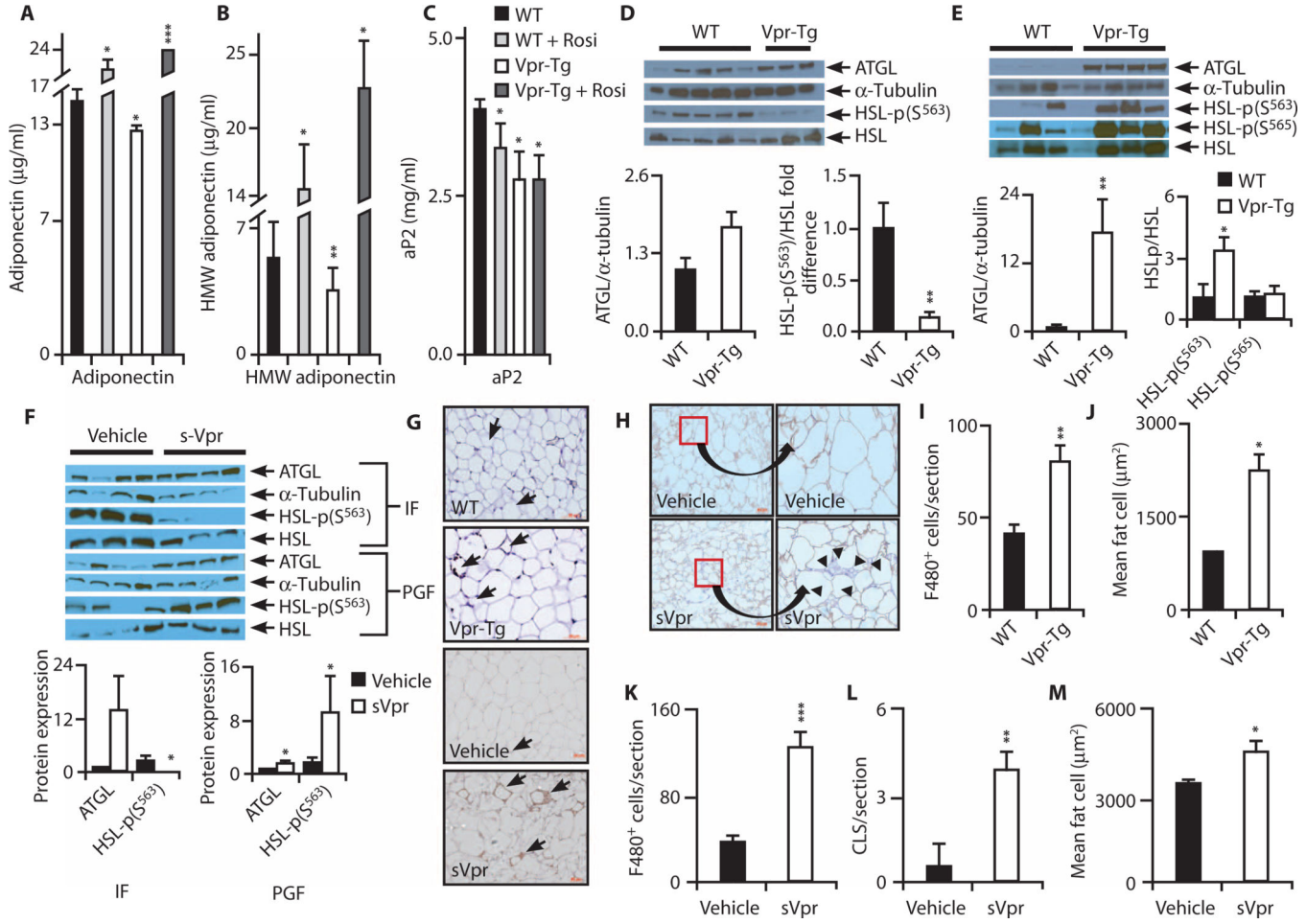


**Fig. 4. Adipokines, lipolytic enzymes, and adipose inflammation in Vpr mice**

(**A** and **B**) Reduced plasma total ($P = 0.04$) and HMW ($P = 0.01$) adiponectin in Vpr-Tg. $n = 5$ per group. (**C**) Reduced plasma aP2 in Vpr-Tg ($P = 0.03$). $n = 5$ for WT and rosiglitazone-treated mice; $n = 8$ for Vpr-Tg. (**D**) ATGL in Vpr-Tg compared to WT IF ($P = 0.06$), and decreased ratio of phospho-HSL ($Ser^{563}$) to total HSL protein in Vpr-Tg ($n = 3$) compared to WT ($n = 5$) IF ($P = 0.02$). Immunoblots are shown above bar graphs. (**E**) Increased ATGL in Vpr-Tg PGF ($n = 4$ per group; $P = 0.01$); increased ratio of phospho-HSL ($Ser^{563}$) to HSL ($P = 0.05$) but not of phospho-HSL ($Ser^{565}$) to HSL in Vpr-Tg ($n = 3$) compared to WT ($n = 5$) PGF. (**F**) ATGL in sVpr-treated compared to water-treated IF ($P = 0.08$), and decreased ratio of phospho-HSL ($Ser^{563}$) to HSL in sVpr-treated IF ($n = 4$ per group; $P = 0.02$). Increased ATGL and increased ratio of phospho-HSL ($Ser^{563}$) to HSL in PGF of sVpr-treated mice ($n = 4$ per group; $P = 0.04$). (**G**) $F4/80^+$ macrophages in PGF of Vpr-Tg (×40) and sVpr-treated mice (×20). Arrows indicate macrophages and crown-like structures (CLSs). (**H**) $F4/80^+$ macrophages and perilipin in PGF of sVpr-treated compared to water-treated mice [×20, cropped and expanded to demonstrate absent perilipin staining (arrowheads) adjacent to CLSs]. (**I**) Increased $F4/80^+$ macrophages in Vpr-Tg PGF. $n = 9$ sections from three mice per group ($P = 0.003$). (**J**) Increased adipocyte size in Vpr-Tg mice ($P = 0.04$). (**K** and **L**) Increased $F4/80^+$ macrophages ($P = 0.0002$) and CLSs in PGF ($P = 0.006$) of sVpr-treated mice ($n = 9$ sections from four mice per group). (**M**) Increased adipocyte size in sVpr-treated mice ($P = 0.03$). Values are means ± SE. $^*P < 0.05$, $^{**}P < 0.01$, $^{***}P < 0.001$ compared to WT.

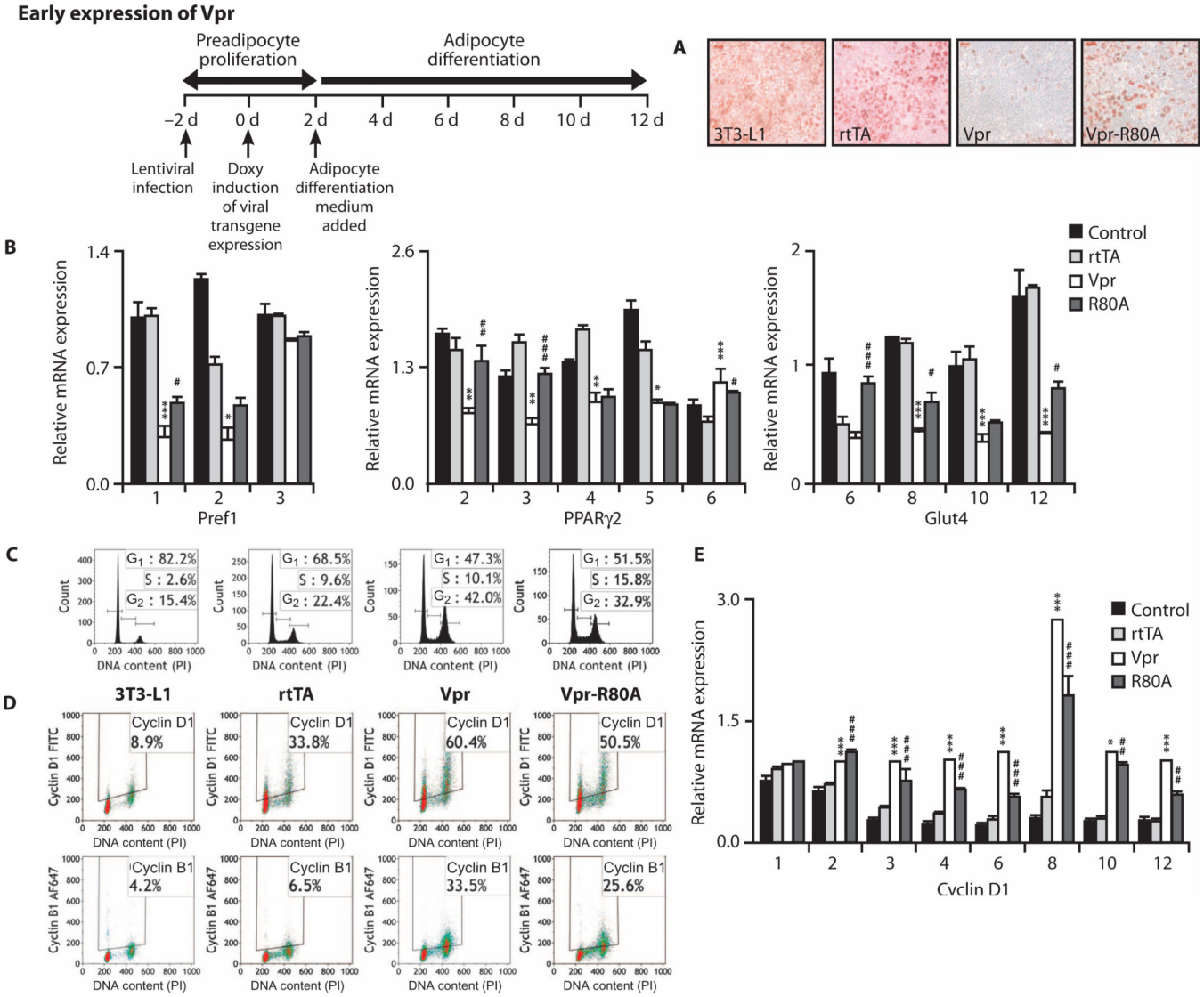


**Fig. 5. Vpr blocks differentiation in 3T3-L1 preadipocytes**

(**A**) Oil Red O staining in 3T3-L1 preadipocytes 10 days after doxycycline. Timeline indicates chronology of lentivirus infection, doxycycline addition (early), and differentiation medium addition. Vpr prevented lipid accumulation, attenuated with Vpr-R80A. (**B**) Expression of *Pref1*, *Pparγ*, and *Glut4* mRNA in preadipocytes on stated days after doxycycline. Vpr reduced the expression of differentiation genes, attenuated with Vpr-R80A. (**C**) Cell cycle histograms of preadipocytes 24 hours after doxycycline (day 1). Vpr caused arrest at $G_2$-M, attenuated with Vpr-R80A. (**D**) Vpr caused accumulation of cyclins D1 and B1 in the preadipocytes, attenuated with Vpr-R80A. (**E**) Vpr caused persistent elevation of Ccnd1 (cyclin D1) mRNA expression in preadipocytes. 3T3-L1, no lentivirus; rtTA, infected with control virus; Vpr, infected with WT-Vpr virus; Vpr-R80A, infected with Vpr R80A virus. Values are means ± SE. **P* < 0.05, ***P* < 0.01, ****P* < 0.001 (comparison between rtTA and Vpr); #*P* < 0.05, ##*P* < 0.01, ###*P* < 0.001 (comparison between Vpr and R80A).

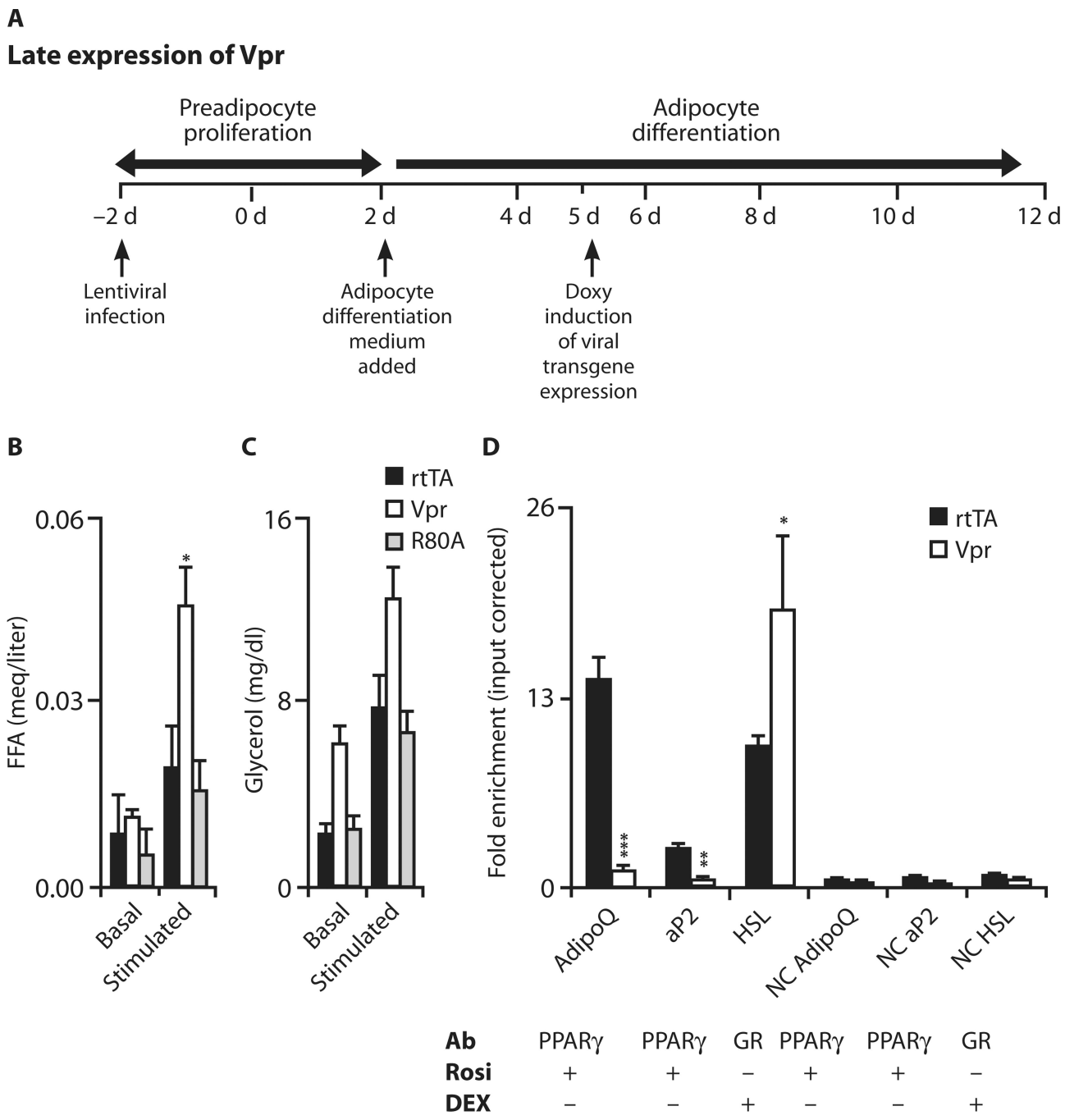


**Fig. 6. Vpr increases lipolysis in adipocytes**

(**A**) Timeline indicates chronology of lentivirus infection, differentiation medium addition, and doxycycline addition (late). (**B** and **C**) Lipolysis (FFA and glycerol release), basal and after stimulation with vehicle or CL316243 (β3-adrenoceptor agonist), in 3T3-L1 cells 72 hours after doxycycline. Vpr increased FFA release ($P = 0.05$). (**D**) Quantification of PPARγ- or GR-associated sequences of *AdipoQ*, *Ap2*, and *Hsl* after ChIP of PPARγ or GR after rosiglitazone or dexamethasone treatment 24 hours after doxycycline. Data are representative of three experiments. Binding site levels of *AdipoQ* ($P = 0.001$) and *Ap2* ($P = 0.01$) were lower, and that of *Hsl* ($P = 0.004$) was higher, in Vpr compared to control (rtTA) condition. Off-target DNA sequences ~2 kb upstream of the PPARγ/GR-binding sites were amplified as negative controls (NC). 3T3-L1, no lentivirus; rtTA, infected with

control virus; Vpr, infected with WT-Vpr virus; Vpr-R80A, infected with Vpr-R80A mutant virus. Values are means ± SE. *$P$ < 0.05, **$P$ < 0.01, ***$P$ < 0.001.

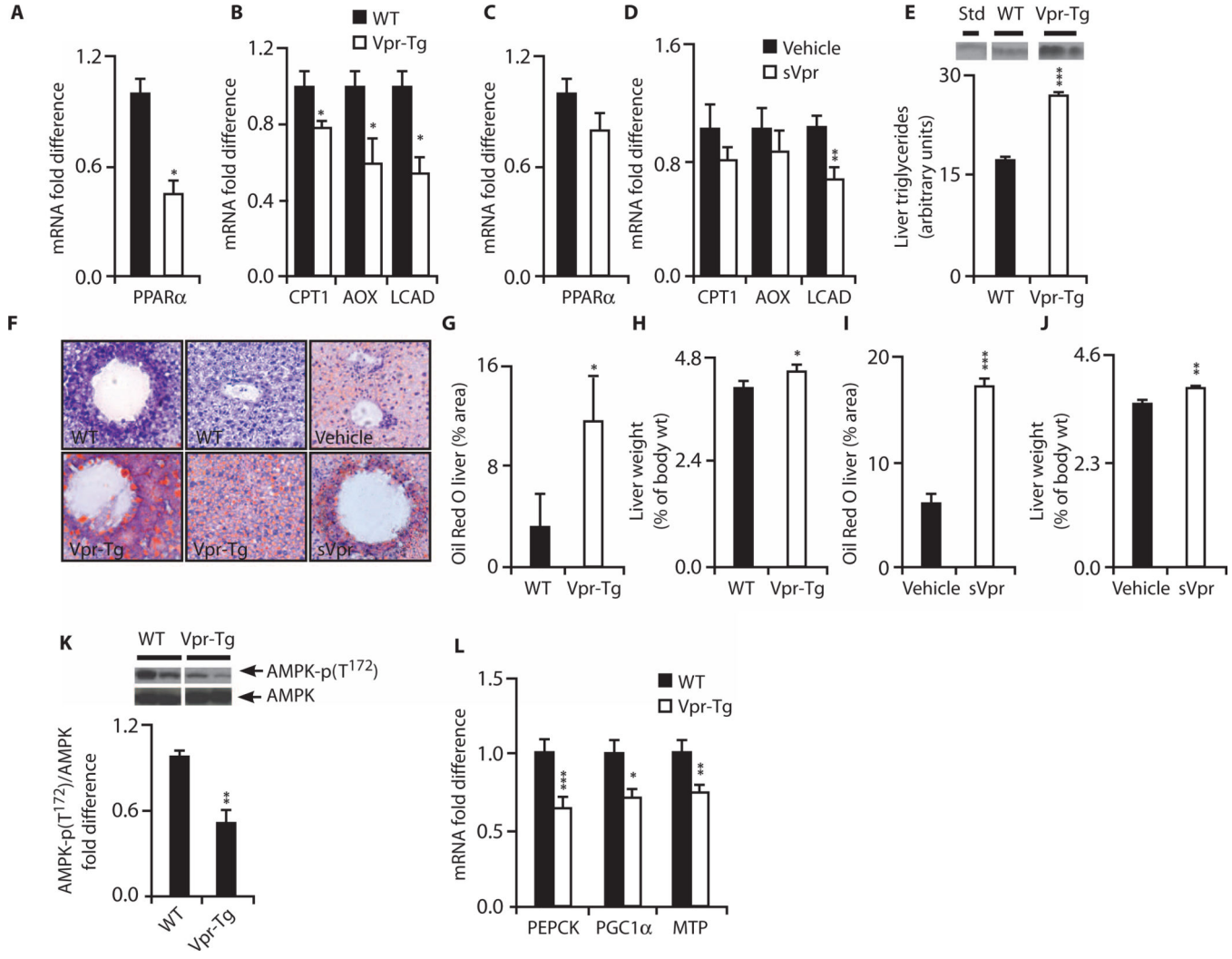


**Fig. 7. Hepatosteatosis and altered hepatic expression of PPARα-regulated oxidative genes in Vpr-Tg and sVpr-treated mice**

(**A**) Reduced *Pparα* mRNA in Vpr-Tg (n = 8 per group; $P = 0.03$). (**B**) Reduced mRNA of *Cpt1α* ($P = 0.05$), *Aox* ($P = 0.02$), and *Lcad* ($P = 0.03$) in Vpr-Tg ($n = 8$ per group). (**C**) *Pparα* mRNA in sVpr-treated compared to water-treated mice ($n = 8$ per group). (**D**) mRNA of *Lcad* ($P = 0.009$), Cpt1α, and *Aox* in sVpr-treated mice ($n = 8$ per group). (**E**) Increased liver triglyceride content in Vpr-Tg ($n = 3$ per group, $P = 0.0005$). (**F**) Oil Red O–stained liver sections of Vpr-Tg compared to WT mice and sVpr-treated compared to water-treated mice (×40). (**G**) Increased Oil Red O staining in Vpr-Tg ($n = 6$) compared to WT ($n = 4$) liver ($P = 0.05$). (**H**) Increased liver mass (normalized to body weight) in Vpr-Tg ($n = 4$ per group; $P = 0.05$). (**I**) Increased Oil Red O staining in liver of sVpr-treated mice ($n = 6$ per group; $P = 0.0001$). (**J**) Increased liver mass (normalized to body weight) in sVpr-treated mice ($n = 8$ per group; $P = 0.004$). (**K**) Reduced ratio of phosphorylated AMPK to total AMPK in Vpr-Tg ($n = 5$) compared to WT ($n = 4$) liver ($P = 0.01$). (**L**) Decreased *Pepck* ($P = 0.001$), *Pgc1α* ($P = 0.04$), and Mtp (P = 0.008) mRNA in liver of Vpr-Tgmice ($n = 8$ per group). Values are means ± SE. *$P < 0.05$, **$P < 0.01$, ***$P < 0.001$.

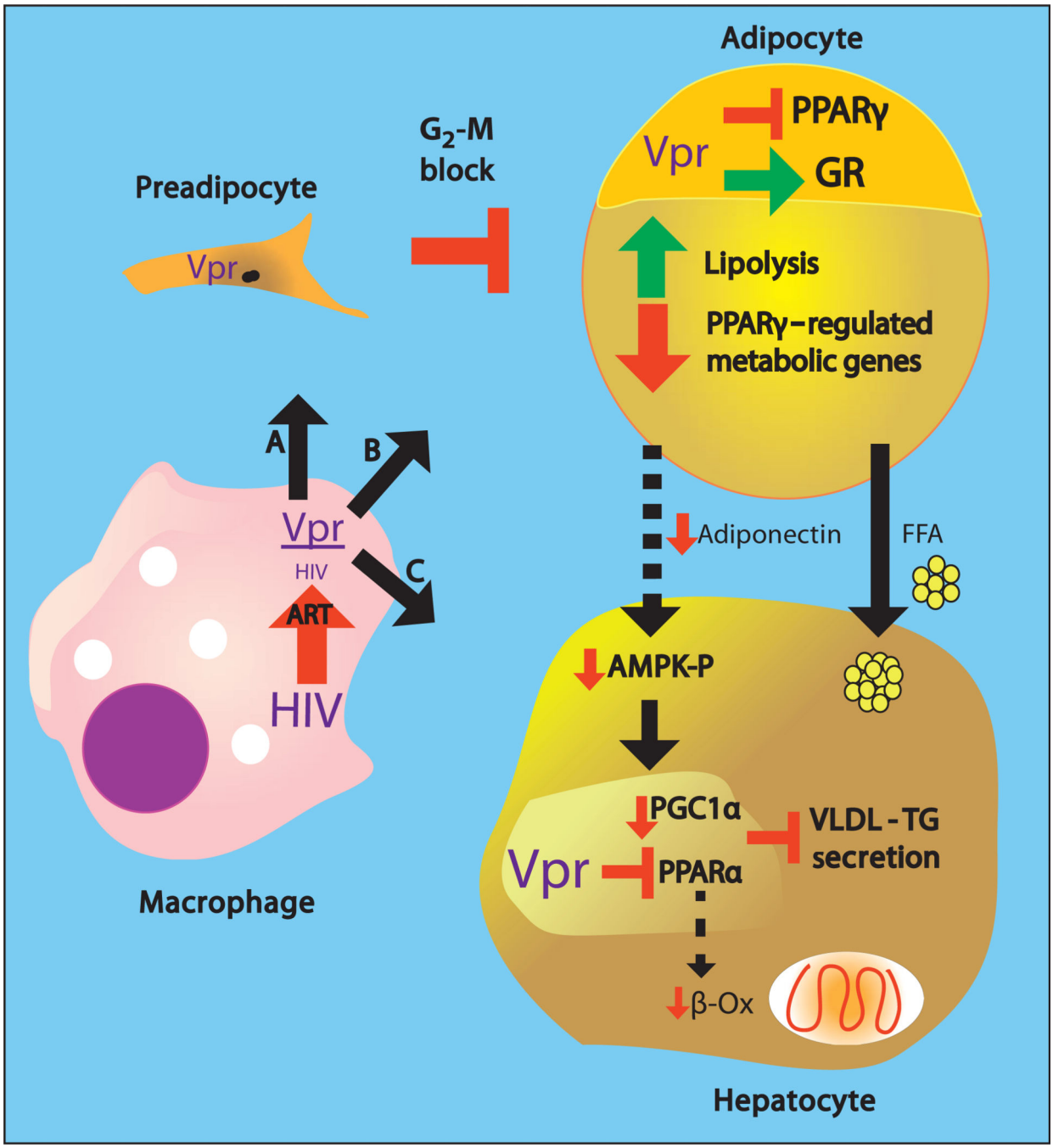


**Fig. 8. Vpr-mediated pathogenesis of HIV-associated metabolic defects**

HIV persisting in tissue macrophages or sequestered T cells after ART releases Vpr that transduces and affects preadipocytes, adipocytes, and hepatocytes. (**A**) In preadipocytes, Vpr blocks the cell cycle at $G_2$-M, blunting turnover and differentiation into adipocytes. (**B**) In mature adipocytes, Vpr co-represses PPARγ-regulated genes and coactivates GR-regulated genes, leading to lipolysis, defective fatty acid storage and metabolism, and diminished secretion of adiponectin. (**C**) In hepatocytes, Vpr co-represses PPARa, leading to defective fat oxidation and blunted VLDL-triglyceride packaging and export. Hepatic consequences

secondary to Vpr's adipocyte effects include increased fatty acid flux and blunted activation of AMPK because of decreased adiponectin, leading to diminished PGC1α expression. Collectively, the direct and secondary hepatic effects lead to fatty liver.